Erciyes University Journal of Institue Of Science and Technology

Research Article
10.65520/erciyesfen.1933774

Imprint:
Volume: 42(2)
Year: 2026
Page: 799-819

Aslı Durmuşoğlu[a*]
Şahin Yıldırım[b]

[a] Asst. Prof., Hakkari University,
aslidurmusoglu@hakkari.edu.tr
[b] Prof., Erciyes University,
sahiny@erciyes.edu.tr

[*] Corresponding Author

Received: 4/19/2026
Accepted: 7/17/2026

Citation:
Aslı Durmuşoğlu, Şahin Yıldırım, (2026). Analysis Of Load Transfer Mechanisms and Structural Performance in Aircraft Landing Gear Systems. *Erciyes University Journal of Institue Of Science and Technology*, 42(2), 799-819. https://doi.org/10.65520/erciyesfen.1933774

Screened by iThenticate for Authors & Researchers

Analysis Of Load Transfer Mechanisms and Structural Performance in Aircraft Landing Gear Systems

Abstract

In the first touchdown phase, aircraft landing gear systems experience highly transient impact loads. Complex internal force transfer mechanisms govern the structural response of the landing gear assembly. Accurate understanding of the transient reaction forces is important for the understanding of the load redistribution characteristics and the identification of the structurally critical regions within multi-link landing gear mechanisms.In the present study, a planar rigid-body multi-body dynamics (MBD) model of a passenger aircraft rear landing gear mechanism was developed to investigate internal reaction-force transmission behavior during loading conditions induced by initial touchdown. The main goal of the study is not to recreate the entire shock absorption process of the landing gear system but to investigate the dominant load transfer paths and transient member-level reaction forces taking place in the initial impact phase. The extracted reaction forces from the MBD model were then used for preliminary structural assessment using finite element analysis (FEA).Transient distributions of reaction forces on the main strut, lateral members, and locking links were computed in order to characterize the hierarchical load transfer behavior within the landing gear assembly. Along with the representative transient peak loading conditions, comparative structural assessments were also performed for titanium and aluminum alloy configurations considering the equivalent stress, total deformation, safety factor, and fatigue-sensitive areas.The results indicate that the main strut and adjacent linkage members are the primary load-transfer path during initial touchdown and that the locking members undergo significant transient axial reaction forces associated with short duration impact redistribution. The comparative structural assessments also reveal that the titanium alloy configuration exhibits reduced levels of deformation and enhanced structural durability attributes when compared to the aluminum alloy model under the examined loading conditions.The study offers an idealized yet physically interpretable context of member-level transient load-transfer behavior and its indicative structural implications for multi-link passenger aircraft landing gear mechanisms.

Keywords: Aircraft landing gear, Multibody dynamics, Internal load transfer, Transient reaction forces, Structural assessment, Fatigue behavior.

Uçak İniş Takımı Sistemlerinde Yük Aktarım Mekanizmalarının ve Yapısal Performansın Analizi

Öz

Uçak iniş takımı sistemleri, inişin başlangıç aşamasında karmaşık iç kuvvet transfer mekanizmalarının iniş takımı montajının yapısal tepkisini yönettiği, son derece geçici darbe yüklerine maruz kalır. Bu geçici tepki kuvvetlerinin doğru yorumlanması, yük yeniden dağılımı özelliklerini anlamak ve çok bağlantılı iniş takımı mekanizmaları içindeki yapısal olarak kritik bölgeleri belirlemek için önemlidir. Bu çalışmada, yolcu uçağı arka iniş takımı mekanizmasının düzlemsel rijit gövde çoklu gövde dinamiği (MBD) modeli, ilk temas kaynaklı yükleme koşulları sırasında iç reaksiyon kuvveti iletim davranışını araştırmak amacıyla geliştirilmiştir. Çalışmanın temel amacı, iniş takımı sisteminin tam şok emme sürecini simüle etmek değil, aksine erken çarpma aşamasında oluşan baskın yük aktarım yollarını ve geçici üye seviyesindeki tepki kuvvetlerini incelemektir. MBD modelinden elde edilen tepki kuvvetleri, daha sonra sonlu elemanlar analizi (FEA) ile ön bir yapısal değerlendirme için kullanıldı. Ana dikme, yan elemanlar ve kilitleme bağlantıları üzerinde etkili olan geçici tepki kuvveti dağılımları, iniş takımı montajı içindeki hiyerarşik yük aktarım davranışını karakterize etmek amacıyla değerlendirildi. Ayrıca, temsil niteliğindeki geçici zirve yükleme koşulları altında eşdeğer gerilme, toplam deformasyon, güvenlik faktörü ve yorulma hassasiyetine sahip bölgeler açısından titanyum ve alüminyum alaşım konfigürasyonları için karşılaştırmalı yapısal değerlendirmeler yapıldı. Sonuçlar, ana direğin ve bitişik bağlantı elemanlarının ilk temas aşamasında birincil yük aktarım yolunu oluşturduğunu, kilitleme elemanlarının ise kısa süreli darbe yeniden dağılımıyla ilişkili önemli geçici eksenel tepki kuvvetleri yaşadığını göstermektedir. Karşılaştırmalı yapısal değerlendirmeler, titanyum alaşımının konfigürasyonunun, incelenen yükleme koşulları altında alüminyum alaşım modeline kıyasla daha düşük deformasyon seviyeleri ve geliştirilmiş yapısal dayanıklılık özellikleri sağladığını göstermektedir. Sunulan çalışma, çok bağlantılı yolcu uçağı iniş takımları mekanizmalarında üye düzeyinde geçici yük aktarım davranışını ve bunun gösterge niteliğindeki yapısal etkilerini araştırmak için idealize edilmiş ancak fiziksel olarak yorumlanabilir bir çerçeve sunmaktadır.

Anahtar kelimeler: Uçak iniş takımı, Çoklu cisim dinamiği, İç yük aktarımı, Geçici reaksiyon kuvvetleri, Yapısal değerlendirme, Yorulma davranışı.

1. INTRODUCTION

Aircraft landing gear systems are among the most critical mechanical structures in aircraft design due to their responsibility for supporting aircraft loads during taxiing, takeoff, and landing operations. During touchdown, landing gear assemblies are subjected to highly transient impact loads generated at the wheel–runway interface. These loads propagate through interconnected structural members, producing complex internal reaction forces, stress concentrations, deformation, and fatigue-sensitive regions within the mechanism. Approximately 85–90% of the total aircraft landing load is transmitted through the main landing gear assemblies, making these components highly critical in terms of structural integrity, operational safety, and service life [1–3].

As aircraft mass, landing velocity, and operational loading requirements continue to increase, accurate characterization of load-transfer behavior and structural response within landing gear systems has become an important aspect of modern aerospace engineering. Previous investigations have demonstrated that the highest stress concentrations and structural demands generally occur in the primary load-carrying members, particularly within the main strut and interconnected support mechanisms forming the dominant load paths during landing events [4–7]. Repeated transient loading conditions may accelerate crack initiation, local stress accumulation, and fatigue-related damage, thereby significantly affecting long-term durability and maintenance requirements.

To investigate these complex dynamic behaviors, multibody dynamics (MBD), finite element analysis (FEA), and flexible multibody dynamics (FMBD) approaches have been extensively utilized in the literature. Early multibody investigations demonstrated the capability of system-level dynamic formulations to capture transient landing responses and internal forceevolution in aircraft landing gear systems [8-13]. In addition, flexible multibody approaches have increasingly been employed to incorporate structural flexibility and improve the physical representation of landing gear dynamics. Xue et al. [14] developed a simplified flexible multibody dynamic model for a main landing gear equipped with flexible leaf springs in order to investigate the influence of structural flexibility on landing behavior. Liu and Wang [15] further improved multibody landing gear simulations by incorporating structural flexibility and bearing contact effects into drop-test analyses. Similarly, Li et al. [16] investigated lever-spring landing gear systems with elastomer shock absorbers through multibody simulations and experimental drop-test evaluations.

Along with the progress of multibody simulation techniques, the development of coupled MBD-FEA methodologies and flexible structural modeling approaches has been parallel and widely established in the field of landing gear research and aerospace structural analysis. Gufler et al. [17] also presented a detailed review of flexible multibody dynamics approaches for engineering design optimization studies. Krasoń and Malachowski [18] compared rigid multibody and three-dimensional finite element models for transport aircraft landing gear systems and showed the importance of coupling dynamic loading behavior with structural analysis. Delprete et al. [19] also proposed a model-based design framework integrating the dynamic and structural analyses for the aircraft landing gear systems. The above studies clearly indicate that the coupling of MBD–FEA and FMBD-based landing gear analyses are already established approaches in the literature. Apart from the dynamic investigations, several studies have been conducted on the structural integrity and fatigue behavior of the landing gear systems under operational loading conditions. Patra and Naik [20] conducted finite element analyses to assess the structural and fatigue safety characteristics of aircraft landing gear systems. Similarly, Aftab et al. [21] studied the structural and fatigue performance of the landing gear structures of passenger aircraft through finite element simulations. Moreover, recent studies have also looked into advanced damping and shock-control mechanisms to improve transient landing response and vibration suppression performance. Kang et al. [22] presented linear and nonlinear landing gear drop simulations with MR dampers and Kang and Choi [23] investigated the structural analysis and shock-control behavior of landing gear systems with MR dampers.

A large body of research exists on coupled MBD-FEA simulations, flexible multibody formulations, and structural landing gear analyses; however, there are few detailed investigations on the transient member-level internal reaction-force evolution and hierarchical load-transfer behavior in simplified multi-link passenger aircraft landing gear mechanisms. Existing studies mainly focus on the global structural response, overall drop-test performance or the system-level dynamic behavior . However, the interpretation of the transient internal load-transfer paths between individual structural members during the initial touchdown stage has been comparatively less discussed. The integrated MBD–FEA approach is increasingly adopted in landing gear studies, but the main applications have been addressed to global structural response prediction, impact-load evaluation, drop-test simulation and design optimization . For instance, Rahmani and Behdinan [5] applied a coupled multibody-finite element approach to evaluate the characteristics of dynamic loading and structural response of landing gear systems. Liu and Wang [15] investigated the landing gear performance by using integrated multibody simulations with structural flexibility effects. On the other hand, the present study is concerned with the interpretation of transient member-level reaction-force evolution and hierarchical load-transfer mechanisms in a six-link passenger-aircraft landing gear configuration. The proposed approach does not aim at the development of a new coupling methodology, but at identifying the dominant force transfer paths and relating these load transfer characteristics to the distributions of deformation, safety-factor and fatigue obtained from the structural analyses.

Therefore, the present study investigates the transient internal load-transfer behavior of a six-link passenger aircraft rear landing gear mechanism under touchdown-induced loading conditions using a planar rigid-body multibody dynamics approach. The primary objective of the study is not to introduce a new MBD–FEA integration framework or to establish a fully coupled flexible landing simulation model, but rather to characterize dominant transient reaction-force paths and member-level load redistribution behavior during the initial touchdown phase. In this context, the adopted planar rigid-body formulation was intentionally simplified to investigate dominant transient load-transfer behavior under conservative initial touchdown conditions rather than the complete shock-absorption dynamics of the landing gear system.The transient reaction forces extracted from the multibody model are subsequently utilized for a preliminary structural assessment of titanium and aluminum alloy configurations through finite element analysis. In this manner, the study aims to provide a physically interpretable evaluation of hierarchical load-transfer mechanisms and their indicative structural implications in multi-link passenger aircraft landing gear systems.

2. MATERIALS AND METHODS

The mechanical behavior of aircraft landing gear systems is governed by highly coupled nonlinear dynamic interactions involving structural components, shock absorbers, and wheel–runway contact forces. To accurately capture these interactions, a physics-based modeling approach grounded in multibody dynamics (MBD) theory is employed. The system dynamics are formulated through coupled differential equations derived from Newton–Euler principles, enabling realistic representation of motion, internal force transmission, and energy dissipation mechanisms.

Appropriate physical idealizations and simplifying assumptions are introduced to preserve the essential dynamic characteristics of the system while maintaining computational efficiency. This modeling strategy allows reliable prediction of transient landing responses and provides detailed time-dependent binding forces acting on each structural member of the landing gear mechanism.

Within this study, the landing gear system is developed as a comprehensive multibody dynamic model to extract kinematic behavior and internal load distributions under representative landing conditions. The resulting force histories are systematically analyzed to identify dominant load-carrying components and hierarchical force transfer pathways within the mechanism, offering direct insight into the mechanical behavior of the landing gear assembly. In addition, the obtained load data were used as input in the structural evaluation, which included deformation and stress analyzes, to examine the structural response of the landing gear system under realistic loading conditions.

The transient reaction-force histories obtained from the MSC Adams simulations were extracted from the principal load-transfer locations of the landing gear mechanism. The updated force–time responses were subsequently evaluated, and the representative peak reaction loads corresponding to the critical touchdown stage were identified. These loads were transferred to the finite element model developed in ANSYS Mechanical and applied directly at the axle connection regions as equivalent external loads. The upper attachment locations of the landing gear assembly were constrained to represent the structural connection to the aircraft fuselage. This procedure enabled direct correlation between the transient load-transfer behavior predicted by the multibody dynamics model and the structural response obtained from the finite element analyses.All translational degrees of freedom at the upper attachment regions of the landing gear assembly were constrained to represent the connection between the landing gear and the aircraft fuselage. The transferred loads were applied at the axle connection locations in the corresponding global coordinate directions obtained from the multibody dynamics simulations.

2.1. Degree of Freedom

The degree of freedom (DOF) of a mechanism represents the number of independent parameters required to completely define the configuration of the mechanism. The DOF depends on the number of links, the number of joints, and the kinematic constraints imposed by the joints. In the present study, the landing gear mechanism was modeled using a planar rigid-body representation in the Y–Z plane in order to investigate the dominant transient load-transfer behavior during the initial touchdown stage.

For planar mechanisms, the degree of freedom can be calculated using Equation (1):

$$F = \lambda(l - j - 1) + \sum_{i}^{j} f_i \tag{1}$$

where λ is the degree of freedom parameter of the space, l is the number of links, j is the number of joints, and fi is the degree of freedom of the i-th joint. Since the present study adopts a planar mechanism formulation, the space parameter was selected as λ = 3.

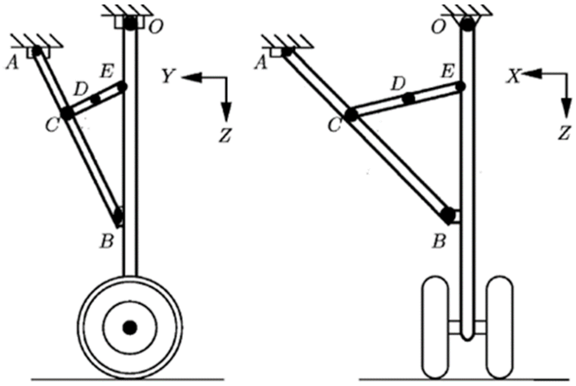

Figure 1. Passenger aircraft main landing gear mechanism front and side view.

Figure 1 illustrates the simplified six-link rear landing gear mechanism of the passenger aircraft considered in this study. The mechanism was represented using planar equivalent joint definitions within the Y–Z plane. Accordingly, the joints were modeled using idealized revolute joint representations consistent with the adopted planar kinematic formulation.Although the landing gear motion was represented in the Y–Z plane for visualization purposes, all kinematic formulations, vector operations, moment calculations, and transient dynamic solutions were evaluated according to the right-hand-rule convention internally employed by the MSC Adams solver environment. The adopted planar representation was therefore used only to simplify visualization and interpretation of the dominant touchdown-induced load-transfer behavior.

$$\lambda = 3\,, l = 6\,, j = 6\,, \sum f_i = 7$$

$$F = 3(6 - 6 - 1) + 7 = 4 \qquad (2)$$

Thus, the landing gear mechanism possesses four degrees of freedom within the adopted planar kinematic representation. These degrees of freedom physically correspond to the dominant planar motions of the interconnected landing gear members during the touchdown event, including the rotational motions of the main linkage components and the associated vertical load-transfer behavior within the Y–Z plane. The adopted planar representation was intentionally selected to investigate the dominant transient reaction-force evolution and internal load-transfer mechanisms during the initial touchdown stage rather than a fully three-dimensional landing simulation including lateral side-load effects. In the present study, the adopted planar rigid-body formulation was intentionally simplified to investigate the dominant transient load-transfer behavior during the initial touchdown stage. Rather than modeling the complete nonlinear oleo-pneumatic shock absorber and tire deformation mechanisms, the dominant compliance and energy dissipation associated with the touchdown event were represented by an equivalent linear spring–damper formulation. This equivalent representation was consistently implemented in both the analytical formulation and the MSC Adams multibody model to ensure methodological consistency while maintaining the computational efficiency of the simplified rigid-body model. Consequently, the extracted reaction forces should be interpreted as representative transient loads corresponding to the initial touchdown phase rather than the detailed response of a fully nonlinear landing gear shock-absorber system.

2.2. Force analysis of the Landing Gear Mechanism

During the initial touchdown phase, the landing gear mechanism is subjected to transient external and internal forces arising from the redistribution of the aircraft weight and the impact-induced reaction at the lower axle region. The linkage members were modeled as rigid bodies, while the dominant compliance and energy dissipation associated with the initial touchdown response were represented by an equivalent linear spring–damper element.

The equivalent force does not represent a detailed nonlinear oleo-pneumatic shock absorber or a separate deformable wheel model. Instead, it accounts for the combined effect of local contact compliance, limited structural flexibility, joint-level deformation, and the dominant dissipative behavior occurring during the early impact phase. The same equivalent stiffness and damping parameters were used in both the analytical formulation and the MSC Adams model.

Force and moment equilibrium equations are systematically formulated for each member of the landing gear mechanism based on the Newton–Euler approach. The corresponding free-body diagrams shown in Figures 2–4 illustrate the external loads, internal reaction forces, and moment equilibrium acting on each rigid limb during the initial touchdown phase.

The equivalent touchdown force is expressed as

$$F_{\mathrm{eq}} = k_{\mathrm{eq}}\delta + c_{\mathrm{eq}}\dot{\delta}, \tag{3}$$

where $k_{\mathrm{eq}}$is the equivalent stiffness coefficient, $c_{\mathrm{eq}}$is the equivalent damping coefficient, $\delta$is the relative displacement at the equivalent load application point, and $\dot{\delta}$ is the corresponding relative velocity.

The equivalent deformation is defined a

$$\delta = z_W - z_{W,0}, \tag{4}$$

and its time derivative is

$$\dot{\delta} = \dot{z}_W, \tag{5}$$

where z_W denotes the vertical displacement of the axle reference point and $z_{W,0}$ is its initial position at the beginning of the touchdown event.

To prevent the equivalent element from generating a tensile force during unloading, the applied force was constrained as

$$F_{\mathrm{eq}} = \max\left[0, k_{\mathrm{eq}}\delta + c_{\mathrm{eq}}\dot{\delta}\right]. \tag{6}$$

For each rigid limb L_i, the translational and rotational equations of motion are written according to the Newton–Euler formulation as

$$\sum F_{iY} = m_i a_{G_iY}, \tag{7}$$
$$\sum F_{iZ} = m_i a_{G_iZ}, \tag{8}$$
$$\sum M_{G_i} = I_{G_i}\ddot{\theta}_i, \tag{9}$$

where m_i, I_{G_i}, a_{G_iY}, a_{G_iZ}, and $\ddot{\theta}_i$ are the mass, mass moment of inertia, translational accelerations, and angular acceleration of limb L_i, respectively.

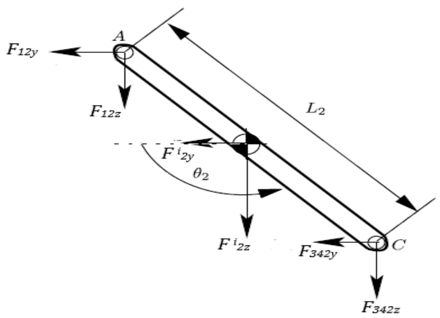

(a)

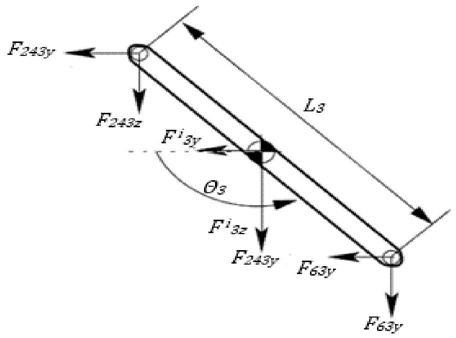

(b)

Figure 2. Free body diagram representations of a) L_2 and b) L_3 links

For limb L_2,

$$F_{12Y} + F_{32Y} = m_2 a_{G_2 Y}, \tag{10}$$
$$F_{12Z} + F_{32Z} + m_2 g = m_2 a_{G_2 Z}, \tag{11}$$
$$\left(\mathbf{r}_{12/G_2} \times \mathbf{F}_{12}\right)_X + \left(\mathbf{r}_{32/G_2} \times \mathbf{F}_{32}\right)_X + M_{12} = I_{G_2} \ddot{\theta}_2. \tag{12}$$

For limb L_3,

$$-F_{32Y} + F_{63Y} = m_3 a_{G_3 Y}, \tag{13}$$
$$-F_{32Z} + F_{63Z} + m_3 g = m_3 a_{G_3 Z}, \tag{14}$$
$$\left(\mathbf{r}_{32/G_3} \times (-\mathbf{F}_{32})\right)_X + \left(\mathbf{r}_{63/G_3} \times \mathbf{F}_{63}\right)_X = I_{G_3} \ddot{\theta}_3. \tag{15}$$

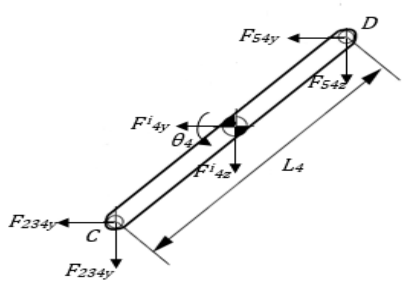

(a)

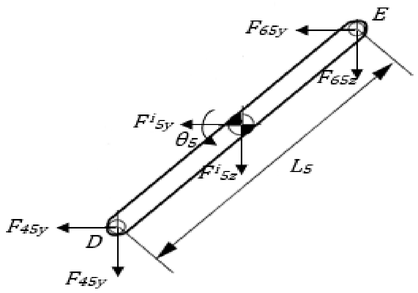

(b)

Figure 3. Free body diagram representations of a) L_4 and b) L_5 links

For limb L_4,

$$F_{34Y} + F_{54Y} = m_4 a_{G_4Y}, \tag{16}$$
$$F_{34Z} + F_{54Z} + m_4 g = m_4 a_{G_4Z}, \tag{17}$$
$$\left(\mathbf{r}_{34/G_4} \times \mathbf{F}_{34}\right)_X + \left(\mathbf{r}_{54/G_4} \times \mathbf{F}_{54}\right)_X = I_{G_4}\ddot{\theta}_4. \tag{18}$$

For limb L_5,

$$-F_{54Y} + F_{65Y} = m_5 a_{G_5Y}, \tag{19}$$
$$-F_{54Z} + F_{65Z} + m_5 g = m_5 a_{G_5Z}, \tag{20}$$
$$\left(\mathbf{r}_{54/G_5} \times (-\mathbf{F}_{54})\right)_X + \left(\mathbf{r}_{65/G_5} \times \mathbf{F}_{65}\right)_X = I_{G_5}\ddot{\theta}_5. \tag{21}$$

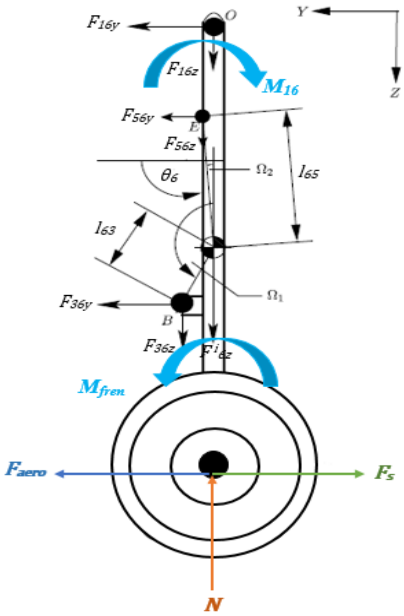

Figure 4. Free body diagram representation of L₆ link

For the primary member L_6, the internal joint reactions, the upper attachment reaction, the external touchdown force, and the equivalent spring–damper force are included as

$$F_{16Y} - F_{63Y} - F_{65Y} + F_{\text{ext},Y} = m_6 a_{G_6Y}, \tag{22}$$
$$F_{16Z} - F_{63Z} - F_{65Z} - F_{\text{eq}} + F_{\text{ext},Z} + m_6 g = m_6 a_{G_6Z}, \tag{23}$$

where the negative sign of F_{eq}results from the downward-positive Z-axis definition.

The rotational equilibrium of L_6 about its mass center is

$$\begin{gathered}\left(\mathbf{r}_{16/G_6} \times \mathbf{F}_{16}\right)_X + \left(\mathbf{r}_{63/G_6} \times (-\mathbf{F}_{63})\right)_X \\ +\left(\mathbf{r}_{65/G_6} \times (-\mathbf{F}_{65})\right)_X + \left(\mathbf{r}_{\mathrm{eq}/G_6} \times \begin{bmatrix} 0 \\ -F_{\mathrm{eq}} \end{bmatrix}\right)_X \\ +M_{16} - M_{\mathrm{brake}} = I_{G_6}\ddot{\theta}_6. \end{gathered} \tag{24}$$

The joint forces satisfy Newton's third law:

$$\mathbf{F}_{23} = -\mathbf{F}_{32}, \tag{25}$$
$$\mathbf{F}_{36} = -\mathbf{F}_{63}, \tag{26}$$
$$\mathbf{F}_{45} = -\mathbf{F}_{54}, \tag{27}$$
$$\mathbf{F}_{56} = -\mathbf{F}_{65}. \tag{28}$$

The dynamic equations of all members can be assembled in matrix form as

$$\mathbf{M}(\mathbf{q})\ddot{\mathbf{q}} + \mathbf{C}(\mathbf{q}, \dot{\mathbf{q}}) + \mathbf{K}_{\mathrm{eq}}(\mathbf{q} - \mathbf{q}_0) + \mathbf{C}_{\mathrm{eq}}\dot{\mathbf{q}} = \mathbf{Q}_{\mathrm{ext}} + \mathbf{Q}_{\mathrm{joint}}, \tag{29}$$

where $\mathbf{M}$ is the mass matrix, $\mathbf{C}$ contains the inertia-related velocity terms, $\mathbf{K}_{\mathrm{eq}}$ and $\mathbf{C}_{\mathrm{eq}}$ represent the equivalent touchdown stiffness and damping contributions, and $\mathbf{Q}_{\mathrm{joint}}$ contains the internal joint reactions.

The internal reaction forces were obtained by simultaneously solving the translational and rotational equations together with the kinematic joint constraints. The peak value of each reaction-force component was determined from

$$F_{ij,\mathrm{peak}} = \max_{t\in[t_c, t_c+\Delta t]} \mid F_{ij}(t) \mid, \tag{30}$$

where $t_c$denotes the initial touchdown time and Δt represents the transient evaluation interval.

The relative difference between the analytical and MSC Adams results was calculated using

$$e_{ij} = \frac{|F_{ij,\mathrm{analytical}} - F_{ij,\mathrm{Adams}}|}{|F_{ij,\mathrm{Adams}}|} \times 100. \tag{31}$$

The mean relative error was obtained as

$$\bar{e} = \frac{1}{n}\sum_{i=1}^{n} e_i\,. \tag{32}$$

The analytical and MSC Adams models were defined using identical mass, inertia, geometric, initial-condition, equivalent stiffness, equivalent damping, and external loading parameters. Consequently, the transient force attenuation observed in the numerical results originates from the damping behavior explicitly included in both formulations.

In Table 1, the structural parameters of the landing gear mechanism are provided.

Table 1. Structural parameters of the landing gear mechanism [24]

Parameter	Value	Parameter	Value
$\mathbf{m_2}$	108 kg	m_6	270 kg
$\mathbf{l_2}$	2220 mm	l_6	2540 mm
$\mathbf{m_3}$	122 kg	θ_2	2,3 rad
$\mathbf{l_3}$	1310 mm	θ_3	2,1 rad
$\mathbf{m_4}$	32 kg	θ_4	0,7 rad
$\mathbf{l_4}$	980 mm	θ_5	0,6 rad
$\mathbf{m_5}$	30 kg	θ_6	1,6 rad
$\mathbf{l_5}$	960 mm	F_{weight}	686,7 kN
$\mathbf{k_{eq}}$	1.5×107 N/m	c_{eq}	4.5×105 Ns/m

3. RESULTS AND DISCUSSION

3.1. Numerical Analysis of the Landing Gear Mechanism

Mechanical systems and virtual experimental environments can be effectively modeled and analyzed using advanced multibody dynamics software. This approach enables realistic simulation of complex mechanical assemblies, allowing detailed investigation of dynamic motion and internal force transmission without reliance on costly physical prototypes or extensive experimental testing. Within the scope of this study, the landing gear mechanism is developed in the MSC Adams environment, where comprehensive binding force analyses are performed to characterize load transfer behavior during landing operation. The geometric configuration of the six-link landing gear mechanism employed in the simulations is illustrated in Figure 5.

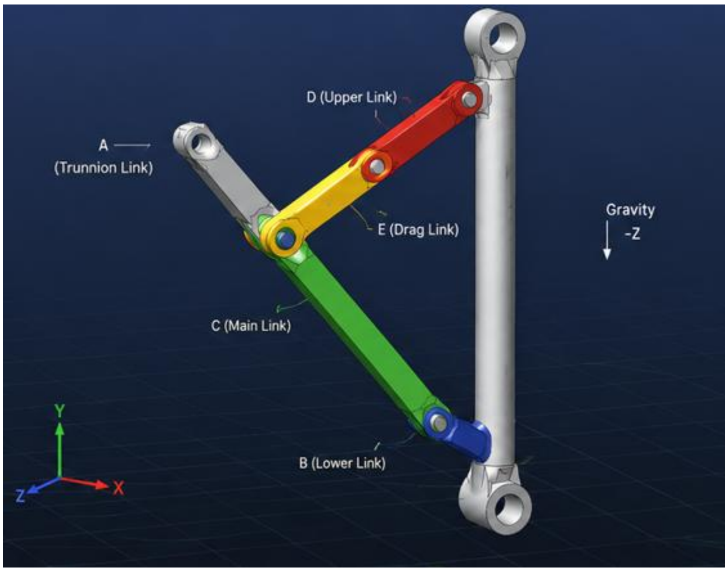

Figure 5. Modeling of the landing gear mechanism in MSC Adams using a planar representation consistent with the right-hand-rule convention.

The limb parameters used in the analytical solution (Table 1) have also been defined in the mechanism model created with Adams. Regarding the force analysis, the graphical representation of the forces and moments occurring at each joint in the landing gear mechanism is provided in Figures 6, 7, 8, 9 and 10.

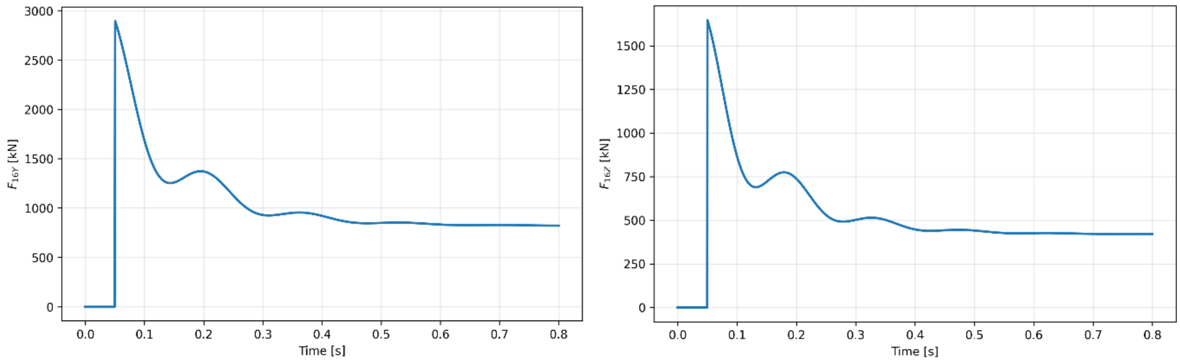

Figure 6. F_{16} bonding force

Figure 6 illustrates the transient reaction-force histories of the F_{16Y} and F_{16Z} components during the initial touchdown stage. Both force components exhibit a rapid impact-induced increase followed by a progressively damped redistribution behavior. The F_{16Z} component reaches a maximum transient force level of approximately 2900 kN immediately after touchdown due to the dominant vertical load-transfer path of the landing gear mechanism, whereas the F_{16Y} component exhibits comparatively lower peak values of nearly 1900 kN together with a faster stabilization behavior. Following the initial impact peak, both force components gradually decrease and converge toward lower transient reaction levels, indicating the redistribution of touchdown-induced loads among the interconnected linkage members. The results further demonstrate that different connection points exhibit distinct transient response characteristics depending on their structural roles and load-transfer functions within the landing gear assembly.

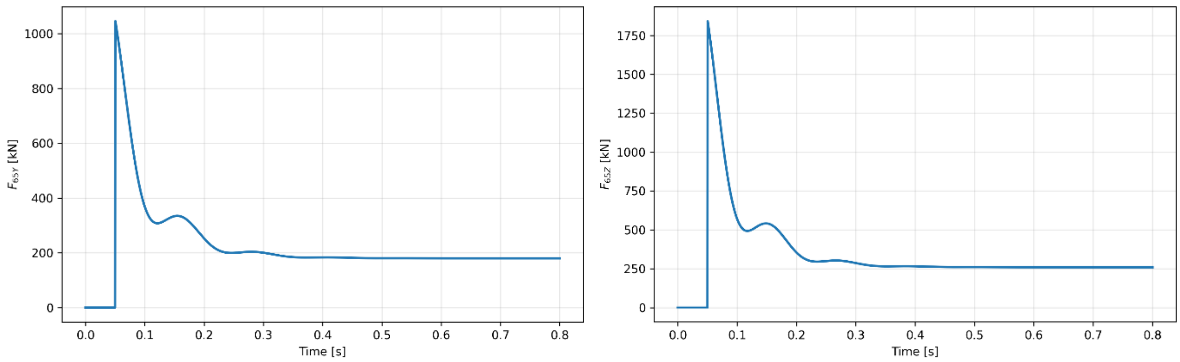

Figure 7. F_{65} bonding force

Figure 7 presents the transient reaction-force histories of the F_{65Y} and F_{65Z} components associated with the secondary locking-link members during the initial touchdown stage. Compared with the primary load-carrying members, the F_{65Y} and F_{65Z} responses exhibit shorter-duration transient peaks and more rapid damping characteristics. The F_{65Z} component reaches a maximum transient force of approximately 1850 kN, while the F_{65Y} component remains at nearly 1050 kN. Following the initial impact transmission, both force components rapidly decrease toward lower transient levels, indicating that the locking-link members primarily participate in short-duration transient load redistribution and temporary impact-force transfer during the early touchdown stage rather than sustained primary load carrying. The obtained responses further indicate that the transient behavior of the secondary linkage region is strongly influenced by the local structural connectivity and the conservative touchdown loading conditions adopted in the present model.

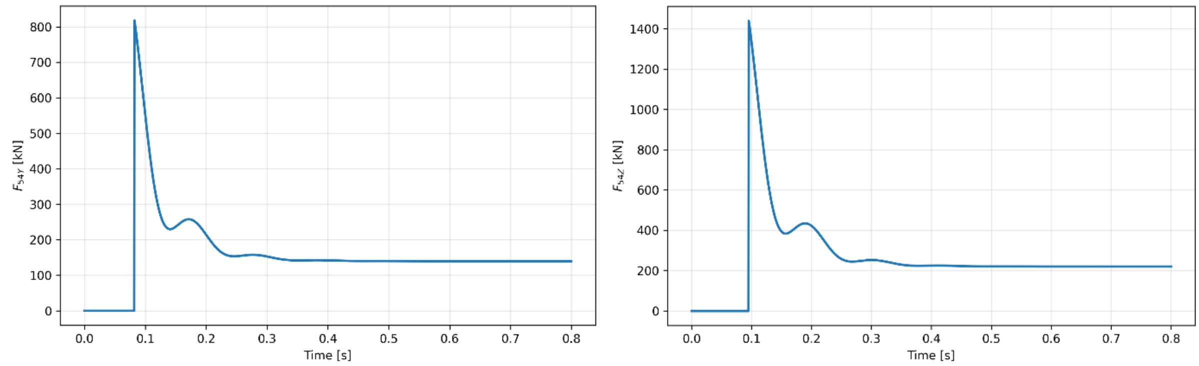

Figure 8. F_{54} bonding force

Figure 8 presents the transient reaction-force histories of the F_{54Y} and F_{54Z} components during the touchdown event. Unlike the primary load-carrying members, the F_{54Y} and F_{54Z} responses exhibit slightly delayed transient peaks, indicating that the corresponding linkage region becomes active after the initial impact-force transmission through the main structural members. The F_{54Z} component reaches a maximum transient force of approximately 1450 kN, whereas the F_{54Y} component remains below nearly 820 kN. Following the transient peak, both force components rapidly decrease toward lower reaction levels, indicating that the associated linkage members primarily participate in short-duration transient load redistribution and temporary force-transfer balancing during the early touchdown stage rather than sustained primary load carrying.

The elevated transient force levels observed in the secondary linkage members correspond primarily to short-duration touchdown-induced reaction-force redistribution during the early impact stage. The reported force components represent global transient reaction-force components obtained from the adopted planar multibody formulation.

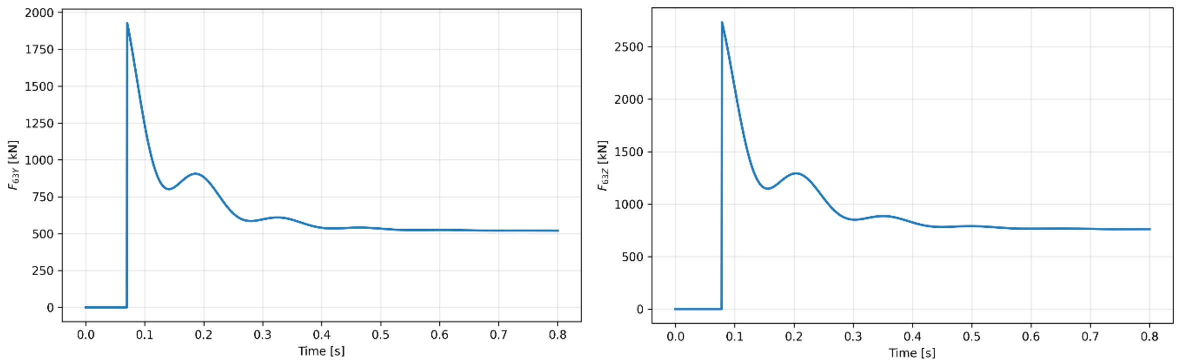

Figure 9. F_{63} bonding force

Figure 9 illustrates the transient reaction-force histories of the F_{63Y} and F_{63Z} components associated with the lateral support region of the landing gear mechanism. Compared with the secondary linkage members, the F_{63} force components exhibit higher transient magnitudes and a relatively longer redistribution duration, indicating a more significant participation in the touchdown-induced load-transfer process. The F_{63Z} component reaches a peak transient force of approximately 2750 kN, while the F_{63Y} component attains nearly 1950 kN during the early impact stage. In contrast to the rapidly decaying responses observed in the locking-link members, the F_{63} responses maintain elevated transient levels for a longer duration, demonstrating the structural contribution of this connection region to the redistribution and transmission of touchdown-induced forces within the main load-transfer path of the landing gear assembly.

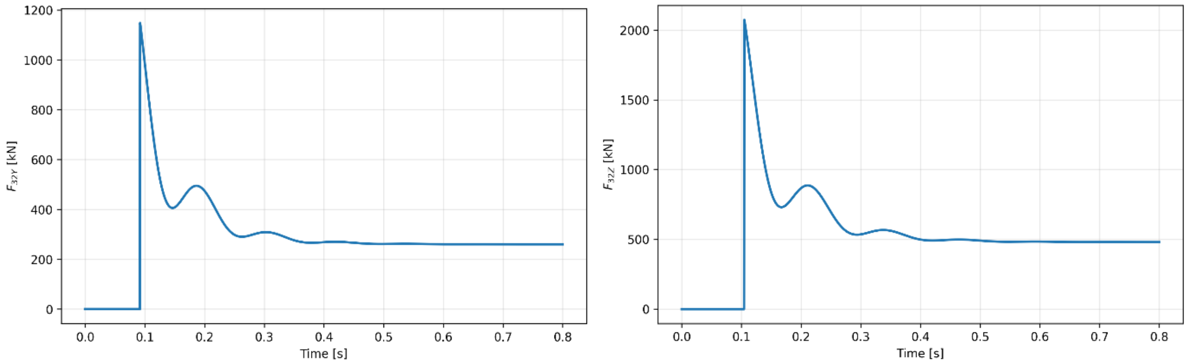

Figure 10. F_{32} bonding force

Figure 10 presents the transient reaction-force histories of the $F_{32Y}$and F_{32Z}components. The responses show a slightly delayed activation compared with the main strut and lateral support regions, indicating that this connection point becomes more effective after the initial impact load has already started to redistribute through the mechanism. The F_{32Z}component reaches a peak value of approximately 2100 kN, whereas the F_{32Y}component remains around 1180 kN. The moderate peak levels and subsequent decay behavior indicate that this member contributes to intermediate load transfer and force balancing between the primary strut path and secondary linkage members during the early touchdown phase.

Table 2. Validation of Analytical and ADAMS Results

Force Component	Analytical Result (kN)	ADAMS Result (kN)	Relative Error (%)
F_{16Z}	2816	2900	2.90
F_{16Y}	1842	1900	3.05
F_{65Z}	1794	1850	3.03
F_{65Y}	1017	1050	3.14
F_{54Z}	1405	1450	3.10
F_{54Y}	793	820	3.29
F_{63Z}	2663	2750	3.16
F_{63Y}	1888	1950	3.18
F_{32Z}	2033	2100	3.19
F_{32Y}	1143	1180	3.14
Average Error	–	–	**3.12**

The validation results obtained using the revised damped analytical formulation are presented in Table 2. Identical geometric properties, mass and inertia parameters, initial conditions, external loading, and equivalent stiffness and damping coefficients were employed in the analytical and MSC Adams models. The relative differences between the peak reaction-force components ranged from 2.90% to 3.29%, with an average relative error of 3.12%. This agreement indicates that the revised analytical formulation consistently reproduces the transient internal load-transfer behavior predicted by the damped multibody dynamics model.

3.2. Fatigue and Stress Deformation Analysis of Landing Gear Mechanism

The finite element method is a prevalent and efficient numerical technique for addressing numerous issues in physics and engineering. The approach depends on modeling intricate structures through smaller, manageable components. The modeling enables the preemption of parameters such as durability, safety, fatigue, noise, and vibration associated with the systems, facilitating the implementation of necessary precautions. The landing gear is a crucial component that supports the aircraft's weight on the ground and experiences various loads during runway landings. These loads can be categorized as fatigue and impact loads. These loads induce axial compression and tension in the landing gear. The deformation analysis of the landing gear was performed utilizing the ANSYS

Workbench software. In finite element method modeling, the model is segmented into fundamental elements comprising smaller components. Consequently, the physical domain is initially partitioned into elements, with the vertices of these elements constituting the point space that represents the physical domain. The results obtained are the values at these specific points.

Figure 11. Landing gear mechanism mesh view

Figure 11 illustrates the finite element mesh structure of the landing gear assembly used in the structural analyses. The model was discretized in ANSYS Mechanical using second-order 10-node tetrahedral elements (SOLID187), which provide improved accuracy for complex geometries and curved structural regions compared with linear tetrahedral formulations. A refined mesh containing approximately 1.0 million elements was generated to accurately capture local stress concentrations and transient load-transfer behavior around the joint regions and geometric transitions. Additional mesh refinement was applied near the upper link–strut connection, lower support regions, and joint interfaces where the peak reaction forces obtained from the ADAMS transient simulations were transferred to the finite element model. A mesh sensitivity assessment was also performed using multiple mesh densities, and the variation in maximum deformation between the medium and fine mesh configurations remained below 2%, indicating mesh-independent structural behavior. Consequently, the adopted mesh density was considered sufficient to provide stable stress distributions and reliable deformation predictions without noticeable numerical artifacts.

Table 3. Mesh sensitivity study of the landing gear finite element model

Mesh Configuration	Number of Elements	Maximum Deformation (mm)
Coarse Mesh	462,318	1.934
Medium Mesh	823,547	1.881
Fine Mesh	1,028,864	1.856

A mesh sensitivity assessment was performed to evaluate the influence of mesh density on the structural response of the landing gear model. Three different mesh configurations, namely coarse, medium, and fine meshes, were analyzed and the corresponding maximum deformation values were compared. As shown in Table 3, the variation in maximum deformation between the medium and fine mesh models remained below 2%, indicating mesh-independent structural behavior. Therefore, the mesh containing approximately 1.2 million elements was selected for all subsequent deformation, safety-factor, and fatigue analyses.

Fatigue-life predictions were performed using the nCode DesignLife module integrated within ANSYS Mechanical. The stress–life (S–N) approach was adopted using the fatigue properties of Ti–6Al–4V and Al7075-T6 alloys. Representative touchdown loads obtained from the multibody dynamics simulations were transferred to the finite element model and applied as constant-amplitude loading conditions. Mean stress effects were accounted for using the Goodman correction model. Fatigue life was evaluated in terms of the predicted number of cycles to failure based on the equivalent stress response of the structure. Since the analysis was based on representative constant-amplitude touchdown loads rather than a variable-amplitude loading spectrum, cycle-counting procedures were not required. This methodology enabled the identification of fatigue-critical regions associated with the dominant load-transfer paths and provided a direct comparison of the fatigue performance of the titanium and aluminum alloy landing gear configurations.

Table 4. Structural parameters of titanium alloy and aluminum alloy

Material Compressive Type	Elasticity Modulud (GPa)	Poisson Rate	Tensile Strenght (MPa)	Strenght (MPa)
Titanium Alloy *(Ti-6Al-4V)*	113	0,34	950	970
Aluminum Alloy *(Al7075T6)*	71,7	0,33	572	482

The material properties employed in the finite element analyses are summarized in Table 4. Titanium alloy (Ti–6Al–4V) and aluminum alloy (Al7075-T6) were selected because they are among the most widely used aerospace structural materials due to their favorable strength-to-weight ratios and proven performance under demanding operational conditions. The comparison of these two materials enables evaluation of the influence of material stiffness and strength characteristics on the deformation behavior, safety factor distribution, and fatigue performance of the landing gear structure under representative touchdown loading conditions.

For both materials, total deformation, fatigue life, and safety factor analyzes under impact loads were conducted. The deformation and safety factor results for titanium and aluminum alloys are shown in Figures 12–15.

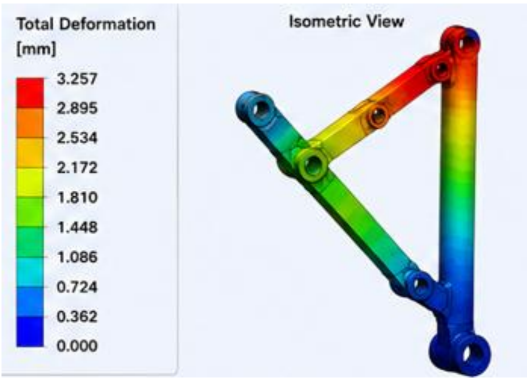

Figure 12. Landing gear total deformation analysis for aluminum alloy material

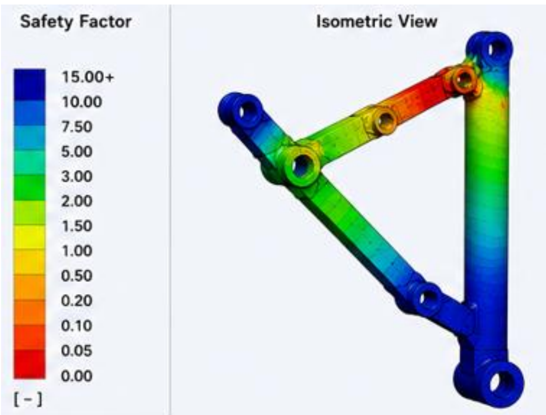

Figure 13. Landing gear factor of safety analysis for aluminum alloy material

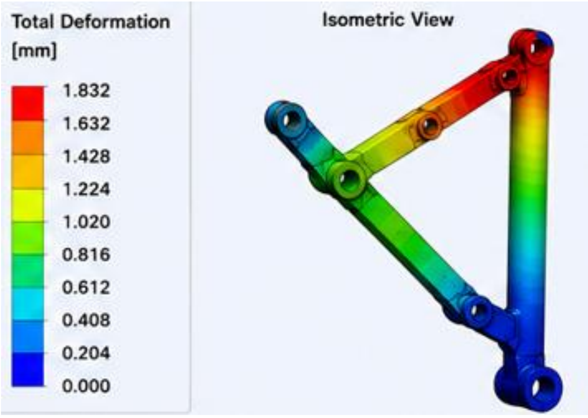

Figure 14. Landing gear total deformation analysis for titanium alloy material

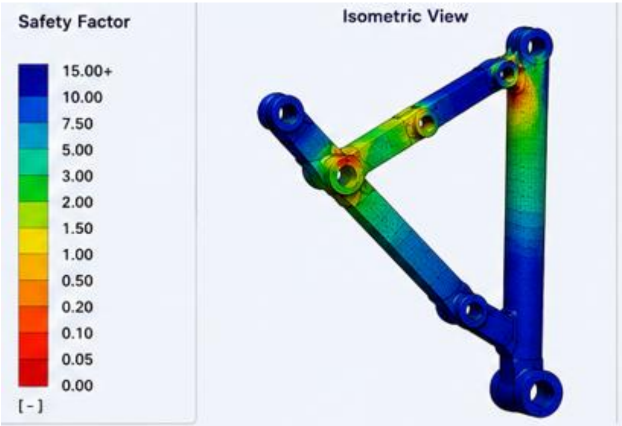

Figure 15. Landing gear factor of safety analysis for titanium alloy material

When a structure is subjected to stress, it deforms, and this deformation varies depending on the type of load and the direction in which it is applied. In this study, the landing gear is primarily deformed under the impact of compressive stresses. The total deformation has been expressed as follows:

$$\Delta L = L_0 - L_1 \tag{33}$$

Figures 12–15 present the total deformation and safety factor distributions obtained for the aluminum and titanium alloy landing gear configurations under the transient touchdown loads transferred from the ADAMS multibody dynamics model. In both material configurations, the maximum deformation and minimum safety factor regions are concentrated around the upper link–strut joint and adjacent linkage interfaces, indicating that these regions constitute the dominant transient load-transfer path during touchdown.

The aluminium alloy model exhibits larger deformations than the titanium alloy configuration due to the lower elastic stiffness of the material. On the other hand, the titanium alloy structure exhibits smaller deformation levels and a more homogeneous structural response under the same loading conditions. The safety factor distributions also show that the localized critical regions are mainly located around the joint transitions and connection interfaces where the bending-induced stress concentrations become dominant. Despite these local concentrations, both material configurations show safety levels that are structurally acceptable under the investigated transient touchdown conditions.

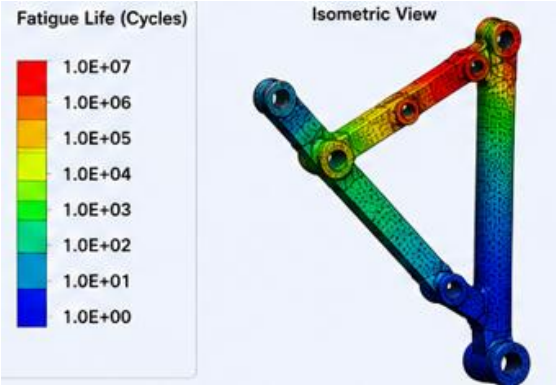

Figure 16. Landing gear fatigue life analysis for aluminum alloy material

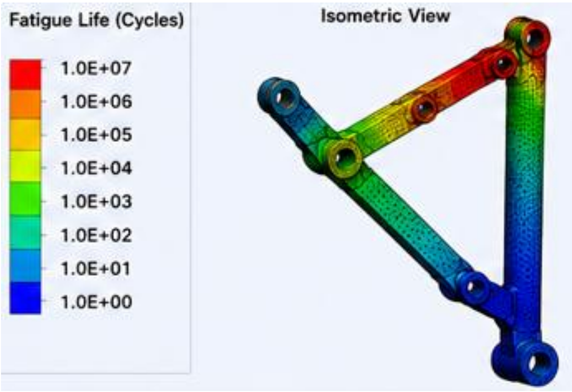

Figure 17. Landing gear fatigue life analysis for titanium alloy material

Figures 16 and 17 show the fatigue life distributions of the aluminum and titanium alloy landing gear models subjected to the transferred transient touchdown loads. The fatigue-sensitive regions are mainly concentrated near the upper joint interfaces and load-transfer regions where repeated transient stress accumulation becomes dominant. The aluminum alloy configuration exhibits comparatively lower fatigue resistance and reduced fatigue life in localized high-stress regions due to the lower material strength and stiffness characteristics.

The titanium alloy configuration showed less deformation, higher safety factors and better fatigue performance than the aluminum alloy configuration but these results should be considered in the context of practical engineering considerations. Titanium alloys generally have higher mechanical strength and fatigue resistance, but these benefits come at the expense of higher material and manufacturing costs. On the other hand, aerospace grade aluminum alloys are still attractive, because of their lower cost, lower density and ease of manufacturability. Therefore, the selection of material for landing gear applications should not be made solely on the basis of structural performance metrics, but should also take into account economic, weight, maintenance and production related factors. The present comparison is meant to demonstrate the importance of material properties on structural response rather than to define a globally better material for all landing gear applications.

4. CONCLUSION

Aircraft landing is a highly transient dynamic event where large reaction forces are generated at the landing gear-runway interface and redistributed through interconnected structural members. In this paper, the force transmission characteristics of a six-link passenger-aircraft rear landing gear mechanism are studied by means of a physics-based multibody dynamics model built in MSC Adams and supported by finite element analyses.

The forces' histories revealed a clear hierarchical structure for load transfer in the landing gear mechanism. The main load carrying components during touchdown were found to be the primary strut and the lateral support members, whereas the locking links were found to be mainly redistributing transient loads and for structural stabilization. The amended force-time responses exhibited large transient peaks immediately after touchdown and then rapid load redistribution in the mechanism. Furthermore, an equivalent linear spring–damper formulation representing the dominant compliance and energy dissipation during the initial touchdown phase was consistently incorporated into both the analytical and MSC Adams models, resulting in physically representative transient force responses.

The transient loads obtained from the multibody dynamics model were then transferred to a finite element framework for structural analysis. Deformation, safety-factor and fatigue-life analyses consistently identified the upper link-strut interfaces, joint regions and the geometric transition zones as the most critical structural locations. The aluminum alloy configuration experienced a maximum deformation on the order of 3.26 mm under the same loading conditions. The titanium alloy configuration resulted in lower deformation and better safety-factor and fatigue-life properties. While titanium had superior structural performance, the actual material selection had to take into account manufacturing costs, weight, maintainability, and production requirements.

The reliability of the developed methodology was verified by comparing selected reaction-force components obtained from the revised analytical formulation with the corresponding results obtained from MSC Adams simulations.The comparison revealed a good agreement between the analytical and numerical methods, with an average relative error of about 3.12%. This agreement confirms the ability of the proposed framework to represent the load-transfer behavior at touchdown with an acceptable accuracy.

Overall, the presented study provides a physically interpretable assessment of transient load-transfer mechanisms and their structural implications in multi-link passenger-aircraft landing gear systems. It should be noted that the present investigation was based on a simplified planar multibody representation and representative touchdown loading conditions. Therefore, three-dimensional structural flexibility, detailed tire–runway interaction effects, advanced shock-absorber fluid dynamics, and variable-amplitude operational loading spectra were not considered within the scope of the study. Future research may focus on fully coupled flexible multibody formulations, more realistic landing scenarios, experimental validation studies, and comprehensive durability assessments under operational loading conditions.

Peer-review: External, Independent.

Acknowledgements:

-

Declarations:

1. Statement of Originality:

This work is original.

2. Author Contributions:

Concept: AD,ŞY; ***Conceptualization:*** AD,ŞY; ***Literature Search:*** AD,ŞY; ***Data Collection:*** AD,ŞY; ***Data Processing:*** AD,ŞY; ***Analysis:*** AD,ŞY; ***Writing – original draft:*** AD,ŞY; ***Writing – review & editing:*** AD,ŞY.

3. Ethics approval:

Not applicable.

4. Funding/Support:

This work has not received any funding or support.

5. Competing Interests:

The authors declare no competing interests.

6. GenAI Usage Statement:

No GenAI tools were used at any stage of the study.

7. Sustainable Development Goals:

REFERENCES

[1] Currey, N. S. (1988). Aircraft landing gear design: Principles and practices. AIAA.

[2] Roskam, J. (2000). Airplane design: Part IV – Layout design of landing gear and systems. DARcorporation.

[3] Milwitzky, B., & Cook, F. E. (1953). Analysis of landing-gear behavior. NACA Technical Report, 1154.

[4] Delprete, C., Dagna, A., & Brusa, E. (2023). Model-Based Design of Aircraft Landing Gear System. Applied Sciences, 13(20), 11465. https://doi.org/10.3390/app132011465.

[5] Rahmani, M., & Behdinan, K. (2018). Dynamic force extraction in aircraft landing gear using multibody simulation. Journal of Aerospace Engineering, 31(4), 04018045. https://doi.org/10.1061/(ASCE)AS.1943-5525.0000856.

[6] Schiehlen, W., & Eberhard, P. (2014). Applied dynamics of multibody systems. Springer. https://doi.org/10.1007/978-3-319-07335-4.

[7] Ghiringhelli, G. L. (2000). Testing of semiactive landing gear control for a general aviation aircraft. Journal of Aircraft, 37(4), 606–616. https://doi.org/10.2514/2.2672.

[8] Shabana, A. A. (2013). Dynamics of multibody systems (4th ed.). Cambridge University Press.

[9] Durmuşoğlu, A. (2021). Analysis and vibration control of passenger aircraft landing gear (Doctoral dissertation). Erciyes University. https://tez.yok.gov.tr/UlusalTezMerkezi/.

[10] Yıldırım, Ş., & Durmuşoğlu, A. (2024). Vibration analysis and control of aircraft landing systems using proposed neural controllers. Neural Computing and Applications, 36(21), 13255-13268. https://doi.org/10.1007/s00521-024-09704-z.

[11] Durmuşoğlu, A., & Yıldırım, Ş. (2025). Vibration Control of Passenger Aircraft Active Landing Gear Using Neural Network-Based Fuzzy Inference System. Applied Sciences, 15(19), 10855.

https://doi.org/10.3390/app151910855.

[12] Gan, S., Fang, X., & Wei, X. (2021). Parametric Analysis on Landing Gear Strut Friction of Light Aircraft for Touchdown Performance. Applied Sciences, 11(12), 5445. https://doi.org/10.3390/app11125445.

[13] Eberhard, P., & Schiehlen, W. (2006). Computational dynamics of multibody systems: history, formalisms, and applications. ASME. J. Comput. Nonlinear Dynamics,1(1):3-12 https://doi.org/10.1115/1.1961875.

[14] Xue, Z. P., Li, M., Li, Y.-H., & Jia, H. G. (2014). A Simplified Flexible Multibody Dynamics for a Main Landing Gear with Flexible Leaf Spring. Shock and Vibration, 2014, 1–10. https://doi.org/10.1155/2014/595964

[15] Liu, W., & Youshan, W. (2024). Improved Multi-Body Dynamic Simulation of Landing Gear Drop Test Incorporating Structural Flexibility and Bearing Contact. Aerospace, 11(7), 543–543. https://doi.org/10.3390/aerospace11070543

[16] Li, F., Zhu, J., Zou, X., Pan, Z., & Chen, J. (2025). Multibody Analysis of Lever-Spring Landing Gear with Elastomer Shock Absorbers: Modelling, Simulations and Drop Tests. Aerospace, 12(5), 367.

[17] Gufler, V., Wehrle, E., & Zwölfer, A. (2021). A review of flexible multibody dynamics for gradient-based design optimization. Multibody System Dynamics, 53(4), 379–409. https://doi.org/10.1007/s11044-021-09802-z

[18] Krasoń, W., & Malachowski, J. (2015). Multibody rigid models and 3D FE models in numerical analysis of transport aircraft main landing gear. Bulletin of the Polish Academy of Sciences Technical Sciences, 63(3), 745–757. https://doi.org/10.1515/bpasts-2015-0086

[19] Delprete, C., Dagna, A., & Brusa, E. (2023). Model-Based Design of Aircraft Landing Gear System. Applied Sciences, 13(20), 11465–11465. https://doi.org/10.3390/app132011465

[20] Patra, P. P., & Naik, J. (2022). Finite Element Analysis of Aircraft Landing Gear for Structural and Fatigue Safety. Zenodo (CERN European Organization for Nuclear Research). https://doi.org/10.5281/zenodo.6951599

[21] Aftab, S. G., Sirajuddin, Sreedhara, B., Ganesh, E., Babu, N. R., & Aithal, S. K. (2021). Finite element analysis of a passenger aircraft landing gear for structural and fatigue safety. Materials Today Proceedings, 54, 152–158. https://doi.org/10.1016/j.matpr.2021.08.199

[22] Kang, B. H., Jo, B.-H., Kim, B.-G., Hwang, J. H., & Choi, S. B. (2023). Linear and Nonlinear Models for Drop Simulation of an Aircraft Landing Gear System with MR Dampers. Actuators, 12(7), 287–287. https://doi.org/10.3390/act12070287

[23] Kang, B. H., & Choi, S. B. (2024). Design, structure analysis and shock control of aircraft landing gear system with MR damper. Smart Materials and Structures, 33(5), 055049–055049. https://doi.org/10.1088/1361-665x/ad3e53

[24] Knowles, J. A., Krauskopf, B., Lowenberg, M. H., Neild, S. A., & Thota, P. (2014). Numerical continuation analysis of a dual-sidestay main landing gear mechanism. Journal of Aircraft, 51(1), 129-143. https://doi.org/10.2514/1.C032130.